Reinforcement Learning-Based Predefined-Time Adaptive Optimized Control for a Two-DOF Helicopter via Event-Triggered Communication

Xiaona Song, *Senior Member, IEEE*, Longbo Chu, Zhijia Zhao, *Member, IEEE*, Keum-Shik Hong, *Life Fellow, IEEE*, Shuai Song, *Member, IEEE*

***Abstract*—This paper focuses on reinforcement learning (RL)-based event-triggered optimized adaptive predefined-time control issue for a two-degree of freedom helicopter system. In the procedure of recursive design, an enhanced predefined-time nonlinear disturbance observer is constructed, which not only enhances the disturbance rejection ability of control system, but also ensures the convergence property of disturbance estimation error. Then, a RL-based optimization strategy with actor-critic-identifier (ACI) structure is incorporated into the predefined-time dynamic surface control framework, which guarantees that approximate optimal control can be achieved. In addition, the communication burden is significantly reduced by using a switching event-triggered mechanism. By utilizing the developed controller, it has been confirmed that all signals in the closed-loop system are practically predefined-time bounded. Finally, the availability and superiority are demonstrated by simulation results by the proposed control method.**

***Index Terms*—Optimized adaptive control, predefined-time disturbance observer, reinforcement learning, switching event-triggered mechanism, two-degree of freedom helicopter system.**

I. Introduction

Unmanned helicopters, as a significant branch of uncrewed aerial vehicles, have been widely utilized in various fields such as logistics and transportation, battlefield reconnaissance, and forest fire prevention attribute to its unique advantages including flexible flight, vertical take-off and landing, and the ability to hover at fixed points [1]–[4]. Nevertheless, the helicopter system, as a typical multiple-input multiple-output (MIMO) nonlinear system, has limited capability of anti-jamming and inherent model uncertainty that seriously threatens the flight performance, or even system stability. As a result, it is essential to enhance the disturbance rejection and robustness of helicopter flight control system design against uncertainties and disturbances [5]–[7].

In practical engineering, it is an indisputable fact that the disturbance is normally difficult to be directly measured. To resolve this situation, numerous control strategies have been researched in recent years. For example, disturbance observer-based tracking control scheme and compensation function observer-based control approach were proposed to weaken the impact of disturbances in [8] and [9], respectively. In [10], the estimation of external disturbances was derived by constructing a second-order disturbance observer. Furthermore, an improved finite-time multivariable neural network disturbance observer was proposed in [11] to solve the formation control issue of multiple uncrewed helicopter systems. Remarkably, Xie et al. [12] adopted a nonlinear disturbance observer to estimate the disturbances. Nevertheless, the above-mentioned documents merely ensure the asymptotic or finite/fixed-time stability of tracking and estimation errors. As of now, there is minimal research on predefined-time nonlinear disturbance observer (PTNDO). Therefore, it is necessary to design a PTNDO for two-degree of freedom (2-DOF) helicopters. In addition, it should be emphasized that a common disadvantage of the above-mentioned results is that they do not take account of the optimal control issue.

An essential part of optimal control is seeking the solution to calculation of the Hamilton-Jacobi-Bellman (HJB) equation [13]. The high nonlinearity characteristic of the HJB equation makes it impossible to derive an analytical solution due to the introduction of uncertainty. To address this problem, finding an approximate solution to the HJB equation online through a reinforcement learning (RL) was discussed in [14]–[16]. Nonetheless, RL is a progressive learning procedure

This work was supported in part by the National Natural Science Foundation of China under Grants 62573178 and 62473130, in part by the Central Plains Talent Program–Leading Talents in Basic Research of Henan Province, in part by the Central Plains Talent Program–Science and Technology Innovation Outstanding Young Talents of Henan Province, in part by the Outstanding Youth Innovation Research Group Project of Natural Science Foundation of Henan Province under Grant 252300421004, in part by the Joint Fund of Science and Technology R&D Plan of Henan Province for Young Scientists under Grant 235200810105, in part by Application Research Project of the Joint Fund of Science and Technology R&D Plan of Henan Province under Grant 242103810052, and in part by the National Research Foundation of Korea funded by the Ministry of Science and ICT, Korea under Grant No. IRIS-2023-00207954. (Corresponding authors: Shuai Song)

Xiaona Song, Longbo Chu, and Shuai Song are with the School of Information Engineering, Henan University of Science and Technology, Luoyang 471000, China (emails: xiaona_97, longbo_2023, songshuai_1010@163.com).

Zhijia Zhao is with the School of Mechanical and Electrical Engineering, Guangzhou University, Guangzhou 510006, China (email: zhjzhaoscut@163.com)

Keum-Shik Hong is with the Institute for Future, School of Automation, Qingdao University, Qingdao 266071, China and also with the School of Mechanical Engineering, Pusan National University, Busan 46241, Korea (email: kshong@pusan.ac.kr)

that unavoidably requires a vast number of training time. To solve this drawback, the actor-critic algorithm was presented, which had been analyzed for its convergence in [17]. At present, some recursive control methods incorporating optimal control strategies [18], [19] have been developed as an effective solution to ensure the stability of dynamic systems. Nevertheless, nonlinear dynamics in practical applications require the processing of a priori knowledge, which makes it difficult to achieve preassigned control objectives. Fortunately, some expert systems with universal approximation have been provided to solve the above-mentioned problems due to their ability to approximate system uncertainty [20], [21]. Nevertheless, the control schemes in previous studies were primarily concentrated on time-triggered mechanism, which may cause the waste of network bandwidth and the increase of system cost.

The event-triggered mechanism (ETM) [22]–[24] can be regarded as an effective approach to investigating the control issues under limited transmission bandwidth. In [24], an adaptive event-triggered neural control strategy was proposed for large-scale system. However, it should be emphasized that the ETM needs to continuously monitor whether events are triggered or not, which imposes some limitations on practical applications. To remove this limitation, self-triggering adaptive control policies [25], [26] were developed for dynamic systems, where the next trigger moment can be computed by means of the current moment information. Additionally, the influence of excessive control gain on the control amplitude has to be addressed with a view to obtaining better control performance. Thus, a decreasing function threshold ETM was proposed in [27], which avoids large controller impulses. However, when the control energy is small, the expected control effect may not be achieved. In this context, in [28], the authors proposed a switching ETM (SETM) method to weigh the foregoing strengths. Nevertheless, the control design with better control behavior for 2-DOF helicopter system (2-DOFHS) under limited communication consumption has not been fully investigated yet.

Despite the finite-time control results [29]–[31], which possess a better steady-state and faster convergence rate, the settling time depends on a priori knowledge of the initial value of the system. In order to overcome this difficulty, the fixed-time convergence concept was proposed and used for the helicopter systems [32]–[34]. However, the upper bound of settling time was seriously impacted by system parameters with regard to fixed time control approach. In this context, the predefined-time control (PTC) concept that upper bound of the settling time depends on the adjustable parameters was presented in [35]. Owing to its advantages, numerous results focused on the PTC have been developed [36]–[39]. In [37], RL-based predefined-time tracking control design for nonlinear servo systems was investigated. In [38], the practically predefined-time (PPT) adaptive fuzzy quantized control was developed, where the robustness of the closed-loop system (CLS) was enhanced by a novel stochastic PTC scheme. Furthermore, the authors in [40] introduced the hyperbolic tangent function to exclude the singularity issue while achieving predefined-time convergence. Despite the significant progress in predefined-time, there are still some research gaps, especially how to realize the predefined-time optimal control of 2-DOFHS with disturbance estimation, which is also a motivation for us to investigate in this study.

Inspired by the aforementioned discussions, this study presents a RL-based event-triggered adaptive predefined-time optimal control approach for a 2-DOFHS. The contributions of this paper are as follows.

1) Distinct from finite/fixed-time control strategies [12], [31], the salient feature of the PTC is that the settling time can be precisely specified by an adjustable parameter in advance, whatever the initial values of the system. Additionally, a PTNDO is proposed for eliminating the effect caused by the lumped disturbance, which also guarantee that the estimation error can converge to zero within a specified time.

2) Compared with the existing recursive control methods [4], [41], [42], this study proposes an amended dynamic surface control design (DSC) involving a predefined-time filter, which not only evades the issue of computational complexity revealed by the traditional backstepping control but also ensures that the predefined-time convergence characteristic of the filter error.

3) An optimized predefined-time DSC framework with ACI structure is established for a 2-DOFHS by utilizing RL to optimize the scheduled cost function, which ensures an approximate trade-off between system performance and control cost can be achieved. In addition, a resource-aware SETM synthesizing the features of self-triggered mechanism [25] and decreasing threshold ETM [27] is developed, which can reduce the consumption of network bandwidth resources without a substantial performance degradation.

Notations: In this article, $\mathrm{tr}\,(\cdot)$ represents the trace of the matrix; $\mathrm{diag}\,\{\cdot\}$ stands for a diagonal matrix; $\|\cdot\|$ represents the Euclidian 2-norm; $\tanh(\cdot)$ denotes the hyperbolic tangent function.

II. System description and preliminaries

A. Model Description

Fig. 1 depicts a simple diagram of a 2-DOFHS [43]. It can be observed from Fig. 1 that the pitch angle θ and yaw angle ϕ of a 2-DOF helicopter are controlled through thrust forces F_p and F_y generated by a pair of DC motors with inputs voltage V_p and V_y. The completeness of this paper, the mathematical expression of the 2-DOF helicopter model is adopted from

[44] as follows:

$$\begin{cases} \ddot{\theta} = \dfrac{-Mgl_a\cos\theta - D_p\dot{\theta}}{(J_p + Ml_a^2)} - \dfrac{Ml_a^2\dot{\phi}^2\sin\theta\cos\theta}{(J_p + Ml_a^2)} \\ \qquad + \dfrac{F_p r_p}{(J_p + Ml_a^2)} + \dfrac{K_{py}F_y r_y}{K_{yy}(J_p + Ml_a^2)}, \\ \ddot{\phi} = \dfrac{-D_y\dot{\phi}}{(J_y + Ml_a^2\cos^2\theta)} + \dfrac{2Ml_a^2\dot{\phi}\dot{\theta}\sin\theta\cos\theta}{(J_y + Ml_a^2\cos^2\theta)} \\ \qquad + \dfrac{F_y r_y}{(J_y + Ml_a^2\cos^2\theta)} + \dfrac{K_{yp}F_p r_p}{K_{pp}(J_y + Ml_a^2\cos^2\theta)}, \end{cases} \tag{1}$$

where ϕ and θ show the yaw and pitch angles, respectively. D_y and D_p stand for the friction coefficients acting on yaw and pitch axes, respectively. J_p and J_y represent the rotary inertias, l_a denotes the distance between the fixed frame origin and the helicopter's center of gravity, K_{pp}, K_{py}, K_{yy}, and K_{yp} represent the thrust torque constants, M indicates the helicopter's total weight, g means the acceleration of gravity. In addition, the thrusts F_p and F_y, resulting from the rotation of the motors, act normal to the fuselage at distances r_p and r_y from the pitch and yaw axes, respectively. These thrusts satisfy the equation $F_p r_p = K_{pp}V_p$ and $F_y r_y = K_{yy}V_y$.

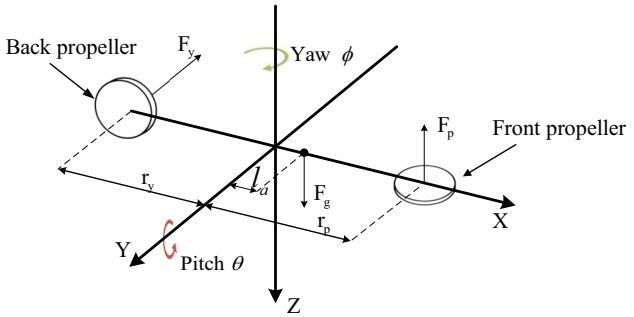

Fig. 1: A simple diagram of the 2-DOF helicopter [43].

Defining $G = [G_1, G_2]^T, G_1 = [\theta, \phi]^T$ and $G_2 = [\dot{\theta}, \dot{\phi}]^T$. Then, the model expression (1) can be rewritten as

$$\begin{cases} \dot{G}_1 = G_2, \\ \dot{G}_2 = H(G) + I(G)u, \\ \quad y = G_1, \end{cases} \tag{2}$$

where $u = [u_1, u_2]^T = [V_p, V_y]^T$ represent the control inputs; and $H(G)$ and $I(G)$ are given by

$$H(G) = \begin{bmatrix} \dfrac{-Mgl_a\cos(G_{11}) - D_p G_{21} - Ml_a^2 G_{22}^2\sin(G_{11})\cos(G_{11})}{J_p + Ml_a^2} \\ \dfrac{-D_y G_{22} + 2Ml_a^2 G_{22}G_{21}\sin(G_{11})\cos(G_{11})}{J_y + Ml_a^2\cos^2(G_{11})} \end{bmatrix},$$

$$I(G) = \begin{bmatrix} \dfrac{K_{pp}}{J_p + Ml_a^2} & \dfrac{K_{py}}{J_p + Ml_a^2} \\ \dfrac{K_{yp}}{J_y + Ml_a^2\cos^2(G_{11})} & \dfrac{K_{yy}}{J_y + Ml_a^2\cos^2(G_{11})} \end{bmatrix}.$$

By taking the external disturbance and system uncertainty into account, the equation (2) is rewritten as

$$\begin{cases} \dot{G}_1 = G_2, \\ \dot{G}_2 = H(G) + I(G)u + \mathcal{D}, \\ \quad y = G_1, \end{cases} \tag{3}$$

where $\mathcal{D}$ denotes the composite disturbance consisting of system uncertainty and unknown disturbance.

B. Radial Basis Function Neural Networks (RBFNNs)

Considering the continuous nonlinear function $\mathbb{F}(x) : R^m \to R$ defined on a compact set $\Omega_x \subset R^m$, its estimation can be derived through the RBFNN approximation satisfying

$$\mathbb{F}(x) = W^T\Phi(x), \tag{4}$$

where x indicates that the input vector, which satisfies $x \in \Omega_x \subset R^m$. In addition, $W \in R^p$ denotes the weight vector, and $\Phi(x) = [\Phi_1(x), \cdots, \Phi_p(x)]^T$ represents the basis function vector that usually is chosen as the Gaussian function with the following form

$$\Phi_i(x) = \exp\left[-\frac{(x - v_i)^T(x - v_i)}{\aleph^2}\right],$$

where v_i denotes the center of the receptive field, and $\aleph > 0$ denotes the width of the basis function. Then, one has

$$\mathbb{F}(x) = W^{*T}\Phi(x) + \Xi(x), \tag{5}$$

where W^* stands for the optimal weight vector, Ξ represents an approximation error satisfying $\|\Xi(x)\| \le \Xi^*$, and $\Xi^* > 0$ is a constant. Furthermore, W^* can be given as [45]

$$W^* = \arg\min_{W\in R^p}\left\{\sup_{x\in\Omega_x}\|\mathbb{F}(x) - W^T\Phi(x)\|\right\}. \tag{6}$$

C. Preliminaries

Assumption 1. The desired reference signal is a continuous smooth bounded function when $t > 0$, and its first-order derivative is also known.

Lemma 1 [46]: For any $\mathcal{A} \in R$, and $\mathcal{B} > 0$, we have

$$0 \le |\mathcal{A}| - \mathcal{A}\tanh(\mathcal{A}/\mathcal{B}) \le 0.2785\mathcal{B}.$$

Lemma 2 [47]: For $\mathcal{X}_1 \in \mathbb{R}$ and $\mathcal{X}_2 \in \mathbb{R}$, it has

$$|\mathcal{X}_1|^{\mathcal{Y}_1}|\mathcal{X}_2|^{\mathcal{Y}_2} \le \frac{\mathcal{Y}_1\jmath}{\mathcal{Y}_1 + \mathcal{Y}_2}|\mathcal{X}_1|^{\mathcal{Y}_1+\mathcal{Y}_2} + \frac{\mathcal{Y}_2\jmath^{\frac{-\mathcal{Y}_1}{\mathcal{Y}_2}}}{\mathcal{Y}_1 + \mathcal{Y}_2}|\mathcal{X}_2|^{\mathcal{Y}_1+\mathcal{Y}_2},$$

where $\mathcal{Y}_1 > 0$, $\mathcal{Y}_2 > 0$, and $\jmath > 0$.

Lemma 3 [48]: For $\aleph_i \in R$, $i \in N^+$, one has

$$\begin{cases} \left(\sum_{i=1}^n |\aleph_i|\right)^m \le \sum_{i=1}^n |\aleph_i|^m, & \text{if } 0 < m < 1, \\ \left(\sum_{i=1}^n |\aleph_i|\right)^m n^{1-m} \le \sum_{i=1}^n |\aleph_i|^m, & \text{if } m > 1. \end{cases}$$

Lemma 4 [49]: For the system $\dot{\mathcal{Z}} = f(t, \mathcal{Z})$. If there exists a predefined time $T_c > 0$ and constant $0 < \pounds < 1$ which makes the Lyapunov function $V(\mathcal{Z})$ fulfill the following inequality:

$$\dot{V} \leq -\frac{\pi}{\pounds T_c \sqrt{\omega_1 \omega_2}}(\omega_1 V^{(2-\pounds)/2} + \omega_2 V^{(2+\pounds)/2}) + \mathcal{N},$$

where $0 < \mathcal{N} < \infty$, ω_1 and ω_2 are positive constants. Additionally, it is obtained that the system is practically predefined-time stable under the settling time $T < T_{max} = \sqrt{2}T_c$. In addition, the system solution residual set is denoted by

$$\left\{ \lim_{t \to T} \mathcal{Z} \mid V \leq \min \left\{ \left(\frac{2\pounds T_c \mathcal{N} \sqrt{\omega_1 \omega_2}}{\pi \omega_1} \right)^{\frac{2}{2-\pounds}}, \left(\frac{2\pounds T_c \mathcal{N} \sqrt{\omega_1 \omega_2}}{\pi \omega_2} \right)^{\frac{2}{2+\pounds}} \right\} \right\}.$$

III. Main Results

A. Predefined-Time Nonlinear Disturbance Observer

First, we introduce an auxiliary system as

$$\dot{\varpi}_1 = H(G) + I(G)u + \rho z_1, \tag{7}$$

where $z_1 = G_2 - \varpi_1$, and $\rho > 0$ stands for a constant.

In addition, a PTNDO can be designed with the following form:

$$\hat{\mathcal{D}} = \rho \hat{z}_1 + \dot{z}_1, \tag{8}$$

where $\hat{\mathcal{D}}$ denotes the disturbance estimation of $\mathcal{D}$, and $\hat{z}_1$ represents the state estimation of z_1 derived by

$$\dot{\hat{z}}_1 = \dot{z}_1 + q_1 \tilde{z}_1^{1-\pounds} \tanh\left(\frac{q_1 \tilde{z}_1^{2-\pounds}}{b} \right) + q_2 \mathrm{sig}^{1+\pounds}(\tilde{z}_1), \tag{9}$$

where $\tilde{z}_1 = z_1 - \hat{z}_1$ denotes the estimation error, $q_1 = \mathbb{A}(\frac{1}{2})^{1-\pounds/2}$, $q_2 = \bar{\mathbb{A}} 2^{\pounds/2} (\frac{1}{2})^{1+\pounds/2}$ with $\mathbb{A} = \frac{\pi \omega_1}{\pounds T_o \sqrt{\omega_1 \omega_2}}$, $\bar{\mathbb{A}} = \frac{\pi \omega_2}{\pounds T_o \sqrt{\omega_1 \omega_2}}$, $q_1 \tilde{z}_1^{1-\pounds} \tanh\left(\frac{q_1 \tilde{z}_1^{2-\pounds}}{b} \right) = \left[q_1 \tilde{z}_{11}^{1-\pounds} \tanh\left(\frac{q_1 \tilde{z}_{11}^{2-\pounds}}{b} \right), q_1 \tilde{z}_{12}^{1-\pounds} \tanh\left(\frac{q_1 \tilde{z}_{12}^{2-\pounds}}{b} \right) \right]^T$, and $\mathrm{sig}^{1+\pounds}(\tilde{z}_1) = \left[|\tilde{z}_{11}|^{1+\pounds} \mathrm{sgn}(\tilde{z}_{12}), |\tilde{z}_{12}|^{1+\pounds} \mathrm{sgn}(\tilde{z}_{11}) \right]^T$, in which $\tanh(\cdot)$ and $\mathrm{sgn}(\cdot)$ are the hyperbolic tangent and sign functions, respectively.

Theorem 1. If the PTNDO (13) in conjunction with parameter update law (14) is constructed, the disturbance estimation error (DEE) $\tilde{\mathcal{D}} = \mathcal{D} - \hat{\mathcal{D}}$ converges within a specified time T_o.

Proof. Select the Lyapunov function as

$$V_o = \frac{1}{2} \tilde{z}_1^T \tilde{z}_1. \tag{10}$$

Differentiating (15) and using Lemma 1 yields

$$\dot{V}_o \leq -\frac{\pi}{\pounds T_o \sqrt{\omega_1 \omega_2}} \left(\omega_1 V_o^{1-\frac{\pounds}{2}} + \omega_2 V_o^{1+\frac{\pounds}{2}} \right) + 0.557b. \tag{11}$$

Then, according to (16) and Lemma 4, it can be obtained that $\tilde{z}_1(t) = 0$ when $t \geq T_o$. Further, calculating the DEE $\tilde{\mathcal{D}}$ gets

$$\tilde{\mathcal{D}} = \mathcal{D} - \rho \hat{z}_1 - \dot{G}_2 + \dot{\varpi}_1 = \rho \tilde{z}_1. \tag{12}$$

Thus, the convergence of the DEE $\tilde{\mathcal{D}}$ can be ensured for $t \geq T_o$. The proof is completed. ■

Remark 1. In contrast to existing disturbance observers presented in [11], [12], the proposed PTNDO guarantees that the DEE strictly converges into a small area around the zero within a predefined time. In addition, the upper bound of the DEE is described by $\lim_{t \to T_o} \tilde{\mathcal{D}} | V_o \leq \min \left\{ \left(\frac{2\pounds T_o 0.557b \sqrt{\omega_1 \omega_2}}{\pi \omega_1} \right)^{\frac{2}{2-\pounds}}, \left(\frac{2\pounds T_o 0.557b \sqrt{\omega_1 \omega_2}}{\pi \omega_2} \right)^{\frac{2}{2+\pounds}} \right\}$, which only relates to the parameters $\pounds, T_o, b, \omega_1$, and ω_2, independent of the system's initial states.

B. Predefined-Time Optimal Control Design with Switching Event-Triggered Mechanism

First, the error variable e_1 and e_2 are defined as

$$\begin{cases} e_1 = G_1 - G_d, \\ e_2 = G_2 - \alpha_f, \end{cases} \tag{13}$$

where G_d is the desired trajectory, and α_f represents the output of the predefined-time filter determined by

$$\xi \dot{\alpha}_f = -w_1 \mathcal{S}^{1-\pounds} \tanh\left(\frac{w_1 \mathcal{S}^{2-\pounds}}{b_1} \right) - w_2 \mathrm{sig}^{1+\pounds}(\mathcal{S}) - \frac{1}{2}\mathcal{S} - \frac{\xi \hat{\sigma}^2 \mathcal{S}}{\sqrt{(\mathcal{S}^T \mathcal{S}) \hat{\sigma}^2 + \Upsilon^2}}, \tag{14}$$

where $\mathcal{S} = \alpha_f - \alpha$ denotes filter error, $\alpha_f(0) = \alpha(0)$, w_1, w_2 are positive constants, satisfying $w_1 = \mathbb{B}(\frac{\xi}{2})^{1-\pounds/2}$, $w_2 = \bar{\mathbb{B}} 5^{\frac{\pounds}{2}} 2^{\pounds} (\frac{\xi}{2})^{1+\pounds/2}$ with $\mathbb{B} = \frac{\pi \omega_1}{\pounds T_c \sqrt{\omega_1 \omega_2}}$, $\bar{\mathbb{B}} = \frac{\pi \omega_2}{\pounds T_c \sqrt{\omega_1 \omega_2}}$. Υ is a positive time-varying parameter.

Noted that the virtual control signal α satisfies the relationship $\|\dot{\alpha}\| \leq \sigma$, in which $\sigma \geq 0$ is an unknown constant. The estimation error can be defined as $\tilde{\sigma} = \sigma - \hat{\sigma}$. $\hat{\sigma}$ denotes the estimation of parameter σ, which can be given by

$$\dot{\hat{\sigma}} = \xi \|\mathcal{S}\| - h_1 \hat{\sigma} - h_2 \hat{\sigma}^{1+\pounds}, \tag{15}$$

where $h_1 = \mathbb{B}^{\frac{2}{2-\pounds}}$, and $h_2 = \bar{\mathbb{B}} \frac{(2+\pounds) 5^{\frac{\pounds}{2}} 2^{\frac{\pounds}{2}}}{2^{1+\frac{\pounds}{2}} (1+\pounds)}$.

Remark 2. In traditional backstepping control approach, the number of differential terms increases dramatically with the increasing of system orders, which is likely to cause the problem of "explosion of complexity". The general DSC strategy overcomes the "explosion of complexity" induced in recursive control by combining the nonlinear filter with backstepping design. However, in the conventional DSC method, the derivative of the virtual control signal α needs to satisfy $|\dot{\alpha}| = B(\cdot)$, which limits the design of the virtual control signals to some extent. In addition, the effect of filter error

on tracking performance is not compensated accordingly. In this work, the characteristic of predefined time convergence is achieved by constructing a nonsingular predefined-time filter (14), which includes the hyperbolic tangent term and parameter updating law (15) while achieving filter error compensation.

Step 1: To obtain the ideal predefined-time optimal virtual controller α^*, it's imperative to minimize the cost function $\mathcal{C}_1 = e_1^T e_1 + \alpha^T \alpha$. Thus, the optimal performance index function $J_1^*(e_1(t))$ can be specified as

$$\begin{aligned} J_1^*(e_1(t)) &= \min_{\alpha \in \Omega_x} \int_t^\infty \left(e_1(\tau)^T e_1(\tau) + \alpha(e_1)^T \alpha(e_1) \right) d\tau \\ &= \int_t^\infty \left(e_1(\tau)^T e_1(\tau) + \alpha^*(e_1)^T \alpha^*(e_1) \right) d\tau, \end{aligned} \tag{16}$$

where Ω_x denotes the set of all allowed control inputs.

According to Bellman's optimality algorithm, the associated HJB equation can be described as

$$\begin{aligned} &\mathcal{H}_1 \left(e_1, \alpha_1^*, \frac{\partial J_1^*}{\partial e_1} \right) \\ =&\|e_1\|^2 + \|\alpha^*\|^2 + \left(\frac{\partial J_1^*}{\partial e_1} \right)^T \dot{e}_1 = 0. \end{aligned} \tag{17}$$

In addition, the optimal virtual controller α^* can be obtained by handing $\partial \mathcal{H}_1 / \partial \alpha^* = 0$

$$\alpha^* = -\frac{1}{2} \frac{\partial J_1^*}{\partial e_1}. \tag{18}$$

To achieve the predefined-time optimal control objective, construct the intermittent cost function as follows:

$$\begin{aligned} J_1^0 =& -2 \left(p_1 e_1^{1-\pounds} \tanh \left(\frac{p_1 e_1^{2-\pounds}}{b_2} \right) + p_2 \mathrm{sig}^{1+\pounds}(e_1) \right) \\ &+ \frac{\partial J_1^*}{\partial e_1} - 3e_1 + 2\dot{G}_d, \end{aligned} \tag{19}$$

where $p_1 = \mathbb{B} \left(\frac{1}{2} \right)^{1-\pounds/2}$ and $p_2 = \bar{\mathbb{B}} 2^{\pounds} 5^{\pounds/2} \left(\frac{1}{2} \right)^{1+\pounds/2}$. Further, one can obtain

$$\begin{aligned} \alpha^* =& -\left(p_1 e_1^{1-\pounds} \tanh \left(\frac{p_1 e_1^{2-\pounds}}{b_2} \right) + p_2 \mathrm{sig}^{1+\pounds}(e_1) \right) \\ &- \frac{1}{2} J_1^0 - \frac{3}{2} e_1 + \dot{G}_d, \end{aligned} \tag{20}$$

$$\begin{aligned} \frac{\partial J_1^*}{\partial e_1} =& 2 \left(p_1 e_1^{1-\pounds} \tanh \left(\frac{p_1 e_1^{2-\pounds}}{b_2} \right) + p_2 \mathrm{sig}^{1+\pounds}(e_1) \right) \\ &+ J_1^0 + 3e_1 - 2\dot{G}_d. \end{aligned} \tag{21}$$

However, the term J_1^0 is unavailable but continuous. Therefore, an actor-critic neural network (ACNN) is utilized to identify J_1^0 such that

$$J_1^0 = W_{s1}^{*T} \Phi_{s1}(X) + \varepsilon_{s1}(X), \tag{22}$$

where $W_{s1}^* = \mathrm{diag} \{ W_{s11}^*, W_{s12}^* \}$ denotes the ideal weight matrix, where $\mathrm{diag}(\cdot)$ stands for a diagonal matrix. $\varepsilon_{s1}(X)$ represents the approximation error vector, which satisfies $\|\varepsilon_{s1}(X)\| \leq \varepsilon_{s1}^*$ with constant $\varepsilon_{s1}^* > 0$. $\Phi_{s1}(X) = [\Phi_{s11}, \Phi_{s12}]^T$ represents the basis function vector with the input vector $X = \left[e_1^T, \dot{G}_d^T \right]^T$.

Here, the ACNN is used to approximate the cost function J_1^0 online, then one gets

$$\begin{aligned} \alpha =& -\left(p_1 e_1^{1-\pounds} \tanh \left(\frac{p_1 e_1^{2-\pounds}}{b_2} \right) + p_2 \mathrm{sig}^{1+\pounds}(e_1) \right) \\ &- \frac{3}{2} e_1 - \frac{1}{2} \hat{W}_{a1}^T \Phi_{s1} + \dot{G}_d, \end{aligned} \tag{23}$$

$$\begin{aligned} \frac{\partial \hat{J}_1}{\partial e_1} =& 2 \left(p_1 e_1^{1-\pounds} \tanh \left(\frac{p_1 e_1^{2-\pounds}}{b_2} \right) + p_2 \mathrm{sig}^{1+\pounds}(e_1) \right) \\ &+ 3e_1 + \hat{W}_{c1}^T \Phi_{s1} - 2\dot{G}_d, \end{aligned} \tag{24}$$

where $\hat{W}_{a1}$ and $\hat{W}_{c1}$ denote the estimation of W_{s1}^*.

Then, the approximation of the HJB equation $\hat{\mathcal{H}}_1(e_1, \alpha, \frac{\partial \hat{J}_1}{\partial e_1})$ is given by

$$\begin{aligned} \hat{\mathcal{H}}_1 =& \left\| -\left(p_1 e_1^{1-\pounds} \tanh \left(\frac{p_1 e_1^{2-\pounds}}{b_2} \right) + p_2 \mathrm{sig}^{1+\pounds}(e_1) \right) \right. \\ &\left. -\frac{3}{2} e_1 - \frac{1}{2} \hat{W}_{a1}^T \Phi_{s1} + \dot{G}_d \right\|^2 + \|e_1\|^2 \\ &+ \left[2 \left(p_1 e_1^{1-\pounds} \tanh \left(\frac{p_1 e_1^{2-\pounds}}{b_2} \right) + p_2 \mathrm{sig}^{1+\pounds}(e_1) \right) \right. \\ &\left. +3e_1 + \hat{W}_{c1}^T \Phi_{s1} - 2\dot{G}_d \right]^T \times (e_2 + \mathcal{S} + \alpha - \dot{G}_d). \end{aligned} \tag{25}$$

Accordingly, the Bellman residual error $\mathcal{E}_1$ is given as

$$\begin{aligned} \mathcal{E}_1 =& \hat{\mathcal{H}}_1 \left(e_1, \alpha, \frac{\partial \hat{J}_1}{\partial e_1} \right) - \mathcal{H}_1 \left(e_1, \alpha_1^*, \frac{\partial J_1^*}{\partial e_1} \right) \\ =& \hat{\mathcal{H}}_1 \left(e_1, \alpha, \frac{\partial \hat{J}_1}{\partial e_1} \right). \end{aligned} \tag{26}$$

Based on the optimal principle, the solution α is expected to ensure that $\mathcal{E}_1$ tends to zero gradually. Considering that the optimal solution is unique, $\hat{\mathcal{H}}_1 = 0$ is equivalent to the following equation also holds:

$$\frac{\partial \hat{\mathcal{H}}_1}{\partial \hat{W}_{a1}} = \frac{1}{2} \Phi_{s1} \Phi_{s1}^T \left(\hat{W}_{a1} - \hat{W}_{c1} \right) = 0. \tag{27}$$

Therefore, the positive function is chosen as

$$E_1 = \frac{1}{2} \left(\hat{W}_{a1} - \hat{W}_{c1} \right)^T \Phi_{s1} \Phi_{s1}^T \left(\hat{W}_{a1} - \hat{W}_{c1} \right). \tag{28}$$

Apparently, the function (27) is equivalent to $E_1 = 0$. Then, the actor-critic learning laws are proposed as

$$\dot{\hat{W}}_{a1} = -w_{a1} \Phi_{s1} \Phi_{s1}^T \left(\hat{W}_{a1} - \hat{W}_{c1} \right), \tag{29}$$

$$\dot{\hat{W}}_{c1} = -w_{c1} \Phi_{s1} \Phi_{s1}^T \hat{W}_{c1} - \frac{1}{2} \Phi_{s1} e_1^T, \tag{30}$$

where w_{a1} and w_{c1} are the defined learning rates.

Select the following Lyapunov function:

$$V_1 = \frac{1}{2}e_1^T e_1 + \frac{\xi}{2}\mathcal{S}^T\mathcal{S} + \frac{1}{2}\tilde{\sigma}^2 + \frac{1}{2}\mathrm{tr}\left(\tilde{W}_{a1}^T\tilde{W}_{a1}\right) + \frac{1}{2}\mathrm{tr}\left(\tilde{W}_{c1}^T\tilde{W}_{c1}\right), \tag{31}$$

where $\mathrm{tr}(\cdot)$ represents the trace of the matrix. $\tilde{W}_{a1} = \hat{W}_{a1} - W_{s1}^*$ and $\tilde{W}_{c1} = \hat{W}_{c1} - W_{s1}^*$.

The derivative of V_1 is

$$\dot{V}_1 = e_1^T(e_2 + \alpha + \mathcal{S} - \dot{G}_d) + \xi\mathcal{S}^T(\dot{\alpha}_f - \dot{\alpha}) - \tilde{\sigma}\dot{\hat{\sigma}} + \mathrm{tr}\left(\tilde{W}_{a1}^T\dot{\hat{W}}_{a1}\right) + \mathrm{tr}\left(\tilde{W}_{c1}^T\dot{\hat{W}}_{c1}\right). \tag{32}$$

Substituting (14), (15), (23), (29) and (30) into (32) and using Lemma 2, one has

$$\begin{aligned}\dot{V}_1 \leq & \frac{1}{2}\|e_2\|^2 - \frac{1}{2}\|e_1\|^2 - \frac{1}{2}e_1^T\hat{W}_{a1}^T\Phi_{s1} - p_2\|e_1\|^{2+\pounds} \\ & - p_1\|e_1\|^{2-\pounds} + h_1\tilde{\sigma}\hat{\sigma} + h_2\tilde{\sigma}\hat{\sigma}^{1+\pounds} - w_1\|\mathcal{S}\|^{2-\pounds} \\ & - w_2\|\mathcal{S}\|^{2+\pounds} + 0.557(b_1+b_2) - \frac{1}{2}\mathrm{tr}\left(\tilde{W}_{c1}^T\Phi_{s1}e_1^T\right) \\ & - w_{a1}\mathrm{tr}\left(\tilde{W}_{a1}^T\Phi_{s1}\Phi_{s1}^T\left(\hat{W}_{a1} - \hat{W}_{c1}\right)\right) + \xi\Upsilon \\ & - w_{c1}\mathrm{tr}\left(\tilde{W}_{c1}^T\Phi_{s1}\Phi_{s1}^T\hat{W}_{c1}\right).\end{aligned} \tag{33}$$

Utilizing the Young's inequality, one can obtain

$$h_1\tilde{\sigma}\hat{\sigma} \leq -\frac{h_1}{2}\tilde{\sigma}^2 + \frac{h_1}{2}\sigma^2. \tag{34}$$

Based on Lemma 2, we have

$$\left(\frac{h_1\tilde{\sigma}^2}{2}\right)^{1-\frac{\pounds}{2}} \leq \mathcal{A}_1(\pounds) + \frac{h_1\tilde{\sigma}^2}{2}, \tag{35}$$

where $\mathcal{A}_1(\pounds) = \frac{\pounds}{2}\left(1-\frac{\pounds}{2}\right)^{\frac{2-\pounds}{\pounds}}$.

According to [50], one yields $x(y-x)^\nu \leq \frac{\nu}{1+\nu}(y^{1+\nu} - x^{1+\nu})$ for $x \leq y$ and $1 < \nu$. Similarly, we can get

$$\tilde{\sigma}\hat{\sigma}^{1+\pounds} \leq \frac{1+\pounds}{2+\pounds}\left(\sigma^{2+\pounds} - \tilde{\sigma}^{2+\pounds}\right). \tag{36}$$

Substituting (34), (35), and (36) into (33) yields

$$\begin{aligned}\dot{V}_1 \leq & \frac{1}{2}\|e_2\|^2 - \frac{1}{2}\|e_1\|^2 - \frac{1}{2}e_1^T\hat{W}_{a1}^T\Phi_{s1} - p_2\|e_1\|^{2+\pounds} \\ & - p_1\|e_1\|^{2-\pounds} + \hbar_1 - \left(\frac{h_1\tilde{\sigma}^2}{2}\right)^{1-\frac{\pounds}{2}} \\ & - \frac{2^{1+\frac{\pounds}{2}}h_2(1+\pounds)}{2+\pounds}\left(\frac{\tilde{\sigma}^2}{2}\right)^{1+\frac{\pounds}{2}} - w_1\|\mathcal{S}\|^{2-\pounds} \\ & - w_2\|\mathcal{S}\|^{2+\pounds} - \frac{1}{2}\mathrm{tr}\left(\tilde{W}_{c1}^T\Phi_{s1}e_1^T\right) \\ & - w_{a1}\mathrm{tr}\left(\tilde{W}_{a1}^T\Phi_{s1}\Phi_{s1}^T\left(\hat{W}_{a1} - \hat{W}_{c1}\right)\right) \\ & - w_{c1}\mathrm{tr}\left(\tilde{W}_{c1}^T\Phi_{s1}\Phi_{s1}^T\hat{W}_{c1}\right),\end{aligned} \tag{37}$$

where $\hbar_1 = 0.557(b_1+b_2) + \xi\Upsilon + \mathcal{A}_1(\pounds) + \frac{h_1}{2}\sigma^2 + h_2\frac{1+\pounds}{2+\pounds}\sigma^{2+\pounds}$.

Step 2: To avoid the unnecessary waste of communication resources, the following SETM is utilized to achieve the transmission of control signal in demand

$$u_i(t) = \mu_i(t_k^i),\ \forall t \in [t_k^i, t_{k+1}^i), i = 1, 2. \tag{38}$$

$$t_{k+1}^i = \begin{cases} t_k^i + \dfrac{\upsilon_i|\mu_i(t)| + \Lambda_i}{\max\{\ell_i, |\dot{\mu}_i(t)|\}}, & |u_i(t)| < L_i, \\ \inf\{t > t_k^i || \chi_i(t)| \geq Q_i, & |u_i(t)| \geq L_i, \end{cases} \tag{39}$$

where $\forall t \geq 0$, $\chi_i(t) = \mu_i(t) - u_i(t)$, $Q_i = \zeta_1 e^{-\zeta_2 t} + \zeta_3$, and t_{k+1}^i denotes the next update time. Moreover, $t_{k+1}^i > t_k^i,\ k \in N^+,\ \ 0 < \upsilon_i < 1, \zeta_1,\ \zeta_2,\ \zeta_3,\ L_i,\ \Lambda_i$ and ℓ_i are the positive constants. Additionally, $\upsilon_i|\mu_i(t)| + \Lambda_i$ stands for the control signal gap from the moment of two consecutive triggered moments. In addition, $|\dot{\mu}_i(t)|$ and ℓ_i denote the change ratios of the control signal gap.

The following two cases are discussed to analyze the SETM.

Case I: If $|u_i(t)| < L_i,\ \mu_i(t)$ is constructed as

$$\mu_i = -(1+\upsilon_i)\left(\hat{u}_i\tanh\left(\frac{e_{2i}\hat{u}_i}{b_3}\right) + \bar{\Lambda}_i\tanh\left(\frac{e_{2i}\bar{\Lambda}_i}{b_3}\right)\right), \tag{40}$$

where $b_3 > 0$ and $\bar{\Lambda}_i > \Lambda_i/(1-\upsilon_i)$, then the time-varying scales φ_{1i} and φ_{2i} meet the condition $\varphi_{1i}, \varphi_{2i} \in [-1, 1]$.

Therefore, one has

$$u_i = \frac{\mu_i - \varphi_{2i}\Lambda_i}{1 + \varphi_{ii}\upsilon_i}. \tag{41}$$

In light of (41) and Lemma 1, one has $e_{2i}u_i \leq -|e_{2i}\hat{u}_i| + 0.557b_3$.

Case II: If $|u_i(t)| \geq L_i,\ \mu_i(t)$ is constructed as

$$\mu_i = -\left(\hat{u}_i\tanh\left(\frac{e_{2i}\hat{u}_i}{b_3}\right) + \zeta_4\tanh\left(\frac{e_{2i}\zeta_4}{b_3}\right)\right), \tag{42}$$

where $b_3 > 0$ and $\zeta_4 \geq \zeta_1 + \zeta_3$, and φ_{3i} is the time-varying scale satisfying $\varphi_{3i} \in [-1, 1]$.

Therefore, one has

$$u_i = \mu_i - \varphi_{3i}Q_i. \tag{43}$$

Based on $-\varphi_{3i}Q_i \leq \zeta_1 + \zeta_3 \leq \zeta_4$ and Lemma 1, one has $e_{2i}u_i \leq -|e_{2i}\hat{u}_i| + 0.557b_3$.

Considering the derivative of e_2, one has

$$\dot{e}_2 = H(G) + I(G)u + \mathcal{D} - \dot{\alpha}_f. \tag{44}$$

Thereafter, the RBFNN is adopted to estimation the $\mathcal{F}(\mathcal{Q}) = H(G)$ with the input vector $\mathcal{Q} = \left[G_1^T, G_2^T\right]^T$. Thus, one obtains

$$\mathcal{F}(\mathcal{Q}) = W^{*T}\Phi(\mathcal{Q}) + \varepsilon(\mathcal{Q}), \tag{45}$$

where $\varepsilon(\mathcal{Q})$ denotes the approximation error and satisfies $\|\varepsilon(\mathcal{Q})\| \leq \varepsilon^*$, and $\varepsilon^* > 0$ is a unknown constant.

Similarly, the optimal performance function can be characterized as

$$\begin{aligned} J_2^*(e_2(t)) &= \min_{u\in\Omega_x} \int_t^\infty \left(e_2(\tau)^T e_2(\tau) + u(e_2)^T u(e_2)\right) d\tau \\ &= \int_t^\infty \left(e_2(\tau)^T e_2(\tau) + u^*(e_2)^T u^*(e_2)\right) d\tau. \end{aligned} \tag{46}$$

Whereafter, the associated HJB equation can be expressed as

$$\begin{aligned} &\mathcal{H}_2\left(e_2, u^*, \frac{\partial J_2^*}{\partial e_2}\right) \\ =&\|e_2\|^2 + \|u^*\|^2 + \left(\frac{\partial J_2^*}{\partial e_2}\right)^T \dot{e}_2 = 0. \end{aligned} \tag{47}$$

Based on $\partial\mathcal{H}_2/\partial u^* = 0$, one has $u^* = -\frac{1}{2} I^T \frac{\partial J_2^*}{\partial e_2}$. Similarly, the intermittent cost function is constructed as

$$\begin{aligned} J_2^0 = \Bigg[&-2\left(p_3 e_2^{1-\pounds}\tanh\left(\frac{p_3 e_2^{2-\pounds}}{b_4}\right) + p_4 \mathrm{sig}^{1+\pounds}(e_2)\right) \\ &+ II^T \frac{\partial J_2^*}{\partial e_2} - 4e_2 - 2\hat{\mathcal{D}} - 2\left(W^{*T}\Phi(\mathcal{Q}) + \varepsilon(\mathcal{Q})\right) \\ &+ 2\dot{\alpha}_f\Bigg], \end{aligned} \tag{48}$$

where $p_3 = \mathbb{B}\left(\frac{1}{2}\right)^{1-\pounds/2}$, and $p_4 = \bar{\mathbb{B}} 2^{\pounds} 4^{\pounds/2}\left(\frac{1}{2}\right)^{1+\pounds/2}$.

Afterward, one can further obtain

$$\begin{aligned} u^* =& I^{-1}\Bigg[-\left(p_3 e_2^{1-\pounds}\tanh\left(\frac{p_3 e_2^{2-\pounds}}{b_4}\right)\right. \\ &\left. + p_4 \mathrm{sig}^{1+\pounds}(e_2)\right) - \frac{1}{2} J_2^0 - \hat{\mathcal{D}} - 2e_2 \\ &- W^{*T}\Phi(\mathcal{Q}) - \varepsilon(\mathcal{Q}) + \dot{\alpha}_f\Bigg], \end{aligned} \tag{49}$$

$$\begin{aligned} \frac{\partial J_2^*}{\partial e_2} =& (I^T)^{-1} I^{-1}\Bigg[2\left(p_3 e_2^{1-\pounds}\tanh\left(\frac{p_3 e_2^{2-\pounds}}{b_4}\right)\right. \\ &\left. + p_4 \mathrm{sig}^{1+\pounds}(e_2)\right) + J_2^0 + 4e_2 + 2\hat{\mathcal{D}} \\ &+ 2\left(W^{*T}\Phi(\mathcal{Q}) + \varepsilon(\mathcal{Q})\right) - 2\dot{\alpha}_f\Bigg]. \end{aligned} \tag{50}$$

By applying an ACNN to function J_2^0 yields

$$J_2^0 = W_{s2}^{*T}\Phi_{s2}(\bar{\mathcal{Q}}) + \varepsilon_{s2}(\bar{\mathcal{Q}}), \tag{51}$$

where $\bar{\mathcal{Q}} = \left[\mathcal{Q}^T, \hat{\mathcal{D}}^T, \mathcal{S}^T, e_2^T\right]^T$ stands for the input vector, $\varepsilon_{s2}(\bar{\mathcal{Q}})$ is the approximation error satisfying $\|\varepsilon_{s2}(\bar{\mathcal{Q}})\| \leq \varepsilon_{s2}^*$.

By employing actor-critic laws to train J_2^0 online yields

$$\begin{aligned} \hat{u} =& I^{-1}\Bigg[-\left(p_3 e_2^{1-\pounds}\tanh\left(\frac{p_3 e_2^{2-\pounds}}{b_4}\right)\right. \\ &\left. + p_4 \mathrm{sig}^{1+\pounds}(e_2)\right) - \frac{1}{2}\hat{W}_{a2}^T\Phi_{s2}(\bar{\mathcal{Q}}) \\ &- 2e_2 - \hat{\mathcal{D}} - \hat{W}^T\Phi(\mathcal{Q}) + \dot{\alpha}_f\Bigg], \end{aligned} \tag{52}$$

$$\begin{aligned} \frac{\partial \hat{J}_2}{\partial e_2} =& (I^T)^{-1} I^{-1}\Bigg[2\left(p_3 e_2^{1-\pounds}\tanh\left(\frac{p_3 e_2^{2-\pounds}}{b_4}\right)\right. \\ &\left. + p_4 \mathrm{sig}^{1+\pounds}(e_2)\right) + \hat{W}_{a2}^T\Phi_{s2}(\bar{\mathcal{Q}}) + 4e_2 \\ &+ 2\hat{\mathcal{D}} + 2\hat{W}^T\Phi(\mathcal{Q}) - 2\dot{\alpha}_f\Bigg], \end{aligned} \tag{53}$$

where $\hat{W}$ denotes the estimated value of W^*. In addition, $\hat{W}_{a2}$, $\hat{W}_{c2}$ denote the esimate values of W_{s2}^*.

Based on the aforementioned steps, the actor-critic learning laws and estimated parameter are designed as

$$\dot{\hat{W}} = \Phi e_2^T - \varrho\hat{W}, \tag{54}$$

$$\dot{\hat{W}}_{a2} = -w_{a2}\Phi_{s2}\Phi_{s2}^T\left(\hat{W}_{a2} - \hat{W}_{c2}\right), \tag{55}$$

$$\dot{\hat{W}}_{c2} = -w_{c2}\Phi_{s2}\Phi_{s2}^T\hat{W}_{c2} - \frac{1}{2}\Phi_{s2}e_2^T, \tag{56}$$

where ϱ, w_{a2} and w_{c2} are the defined parameters.

Select the following Lyapunov function:

$$\begin{aligned} V_2 =& \frac{1}{2}e_2^T e_2 + \frac{1}{2}\mathrm{tr}\left(\tilde{W}_{a2}^T\tilde{W}_{a2}\right) + \frac{1}{2}\mathrm{tr}\left(\tilde{W}_{c2}^T\tilde{W}_{c2}\right) \\ &+ \frac{1}{2}\mathrm{tr}\left(\tilde{W}^T\tilde{W}\right), \end{aligned} \tag{57}$$

where $\tilde{W} = \hat{W} - W^*$, $\tilde{W}_{s2} = \hat{W}_{s2} - W_{s2}^*$ with $s = a, c$.

Using (52), (54)-(56), and the Lemma 3, $\dot{V}_2$ is

$$\begin{aligned} \dot{V}_2 \leq& -w_{a2}\mathrm{tr}\left(\tilde{W}_{a2}^T\Phi_{s2}\Phi_{s2}^T\left(\hat{W}_{a2} - \hat{W}_{c2}\right)\right) \\ &- \varrho\mathrm{tr}\left(\tilde{W}^T\hat{W}\right) - w_{c2}\mathrm{tr}\left(\tilde{W}_{c2}^T\Phi_{s2}\Phi_{s2}^T\hat{W}_{c2}\right) \\ &- \frac{1}{2}\mathrm{tr}\left(\tilde{W}_{c2}^T\Phi_{s2}e_2^T\right) - \frac{1}{2}e_2^T\hat{W}_{a2}^T\Phi_{s2} - p_3\|e_2\|^{2-\pounds} \\ &- p_4\|e_2\|^{2+\pounds} - \|e_2\|^2 + \hbar_2, \end{aligned} \tag{58}$$

where $\hbar_2 = 0.557(2b_3 + b_4) + 0.2785b_3(I_{11} + I_{12} + I_{21} + I_{22}) + \frac{1}{2}\|\varepsilon^*\|^2 + \frac{1}{2}\|\tilde{\mathcal{D}}\|^2$.

C. Stability Analysis

Theorem 2. Consider 2-DOFHS (2) under Assumption 1. If the optimized adaptive control strategy including the predefined-time filter (14), parameter update law (15), virtual controller (23), identifier AC laws (29)-(30) and (54)-(56), the SETM (39), and the predefined-time controller (52) are adopted, the following properties can be ensured:

- All signals in the CLS are practically predefined-time bounded;
- The tracking errors evolve to a small region around the zero within a predefined time;
- Zeno behavior can be evaded.

Proof. Select the Lyapunov function as

$$V = V_1 + V_2. \tag{59}$$

In view of $\hat{W}_{ai} - \hat{W}_{ci} = \tilde{W}_{ai} - \tilde{W}_{ci}$, differentiating (59) yields

$$\begin{aligned} \dot{V} \leq& -p_1\|e_1\|^{2-\pounds} - p_2\|e_1\|^{2+\pounds} - p_3\|e_2\|^{2-\pounds} \\ &- p_4\|e_2\|^{2+\pounds} - w_1\|\mathcal{S}\|^{2-\pounds} - w_2\|\mathcal{S}\|^{2+\pounds} \end{aligned}$$

$$
\begin{aligned}
&-\left(\frac{h_1\tilde{\sigma}^2}{2}\right)^{1-\frac{\pounds}{2}}-\frac{2^{1+\frac{\pounds}{2}}}{2+\pounds}h_2(1+\pounds)\left(\frac{\tilde{\sigma}^2}{2}\right)^{1+\frac{\pounds}{2}}\\
&-\sum_{i=1}^{2}w_{ai}\mathrm{tr}\left(\tilde{W}_{ai}^T\Phi_{si}\Phi_{si}^T\left(\tilde{W}_{ai}-\tilde{W}_{ci}\right)\right)-\sum_{i=1}^{2}\frac{1}{2}\|e_i\|^2\\
&-\sum_{i=1}^{2}w_{ci}\mathrm{tr}\left(\tilde{W}_{ci}^T\Phi_{si}\Phi_{si}^T\hat{W}_{ci}\right)-\sum_{i=1}^{2}\frac{1}{2}\mathrm{tr}\left(\hat{W}_{ci}^T\Phi_{si}e_i^T\right)\\
&-\sum_{i=1}^{2}\frac{1}{2}e_i^T\tilde{W}_{ai}^T\Phi_{si}-\varrho\mathrm{tr}\left(\tilde{W}^T\hat{W}\right)+\hbar_1+\hbar_2. \qquad (60)
\end{aligned}
$$

Applying Young's inequality results in

$$
\begin{aligned}
&w_{ai}\mathrm{tr}\left[\tilde{W}_{ai}^T\Phi_{si}\Phi_{si}^T\left(\tilde{W}_{ai}-\tilde{W}_{ci}\right)\right]\\
\leq&-\frac{w_{ai}}{2}\mathrm{tr}\left(\tilde{W}_{ai}^T\Phi_{si}\Phi_{si}^T\tilde{W}_{ai}\right)\\
&+\frac{w_{ai}}{2}\mathrm{tr}\left(\tilde{W}_{ci}^T\Phi_{si}\Phi_{si}^T\tilde{W}_{ci}\right) \qquad (61)\\
&-\frac{1}{2}\mathrm{tr}\left(\hat{W}_{ci}^T\Phi_{si}e_i^T\right)-\frac{1}{2}e_i^T\tilde{W}_{ai}^T\Phi_{si}\\
\leq&\frac{1}{4}\mathrm{tr}\left(\hat{W}_{ci}^T\Phi_{si}\Phi_{si}^T\hat{W}_{ci}\right)+\frac{1}{2}\|e_i\|^2\\
&+\frac{1}{4}\mathrm{tr}\left(\tilde{W}_{ai}^T\Phi_{si}\Phi_{si}^T\tilde{W}_{ai}\right) \qquad (62)\\
&-\varrho\mathrm{tr}\left(\tilde{W}^T\hat{W}\right)\\
\leq&-\frac{\varrho}{2}\mathrm{tr}\left(\tilde{W}^T\tilde{W}\right)+\frac{\varrho}{2}\mathrm{tr}\left(W^{*T}W^*\right) \qquad (63)
\end{aligned}
$$

In addition, one has

$$
\begin{aligned}
&w_{ci}\mathrm{tr}\left(\tilde{W}_{ci}^T\Phi_{si}\Phi_{si}^T\hat{W}_{ci}\right)\\
=&\frac{w_{ci}}{2}\left(\mathrm{tr}\left(\tilde{W}_{ci}^T\Phi_{si}\Phi_{si}^T\tilde{W}_{ci}\right)+\mathrm{tr}\left(\hat{W}_{ci}^T\Phi_{si}\Phi_{si}^T\hat{W}_{ci}\right)\right.\\
&\left.-\mathrm{tr}\left(W_{ci}^{*T}\Phi_{si}\Phi_{si}^TW_{ci}^*\right)\right) \qquad (64)
\end{aligned}
$$

By defining $\lambda_{min}^{\Phi_{si}}>0$ as the minimum eigenvalue of matrix $\Phi_{si}\Phi_{si}^T$ and choosing the suitable defined scales such that $(w_{ci}-w_{ai})\lambda_{min}^{\Phi_{si}}/2>1,(2w_{ai}-1)\lambda_{min}^{\Phi_{si}}/4>1,(2w_{ci}-1)/4>0,(\varrho/2)>1$ hold, it follows from (60)-(64) that

$$
\begin{aligned}
\dot{V}\leq&-p_1\|e_1\|^{2-\pounds}-p_2\|e_1\|^{2+\pounds}-p_3\|e_2\|^{2-\pounds}\\
&-p_4\|e_2\|^{2+\pounds}-w_1\|\mathcal{S}\|^{2-\pounds}-w_2\|\mathcal{S}\|^{2+\pounds}\\
&-\left(\frac{h_1\tilde{\sigma}^2}{2}\right)^{1-\frac{\pounds}{2}}-\frac{2^{1+\frac{\pounds}{2}}h_2(1+\pounds)}{2+\pounds}\left(\frac{\tilde{\sigma}^2}{2}\right)^{1+\frac{\pounds}{2}}\\
&-\sum_{i=1}^{2}\mathrm{tr}\left(\tilde{W}_{ai}^T\tilde{W}_{ai}\right)-\sum_{i=1}^{2}\mathrm{tr}\left(\tilde{W}_{ci}^T\tilde{W}_{ci}\right)\\
&-\mathrm{tr}\left(\tilde{W}^T\tilde{W}\right)+\hbar_3 \qquad (65)
\end{aligned}
$$

where $\hbar_3=\hbar_1+\hbar_2+\sum_{i=1}^{2}\left(w_{ci}\lambda_{min}^{\Phi_{si}}\mathrm{tr}\left(W_{ci}^{*T}W_{ci}^*\right)\right)/2+\left(\varrho\mathrm{tr}\left(W^{*T}W^*\right)\right)/2$.

Furthermore, one has

$$
\begin{aligned}
-\mathrm{tr}\left(\tilde{W}^T\tilde{W}\right)\leq&-\left(\mathrm{tr}\left(\frac{\tilde{W}^T\tilde{W}}{2}\right)\right)^{1-\frac{\pounds}{2}}\\
&-\left(\mathrm{tr}\left(\frac{\tilde{W}^T\tilde{W}}{2}\right)\right)^{1+\frac{\pounds}{2}}+\wp \qquad (66)\\
-\sum_{i=1}^{2}\mathrm{tr}\left(\tilde{W}_{si}^T\tilde{W}_{si}\right)\leq&-\left(\sum_{i=1}^{2}\mathrm{tr}\left(\frac{\tilde{W}_{si}^T\tilde{W}_{si}}{2}\right)\right)^{1-\frac{\pounds}{2}}+\wp_s\\
&-\left(\sum_{i=1}^{2}\mathrm{tr}\left(\frac{\tilde{W}_{si}^T\tilde{W}_{si}}{2}\right)\right)^{1+\frac{\pounds}{2}} \qquad (67)
\end{aligned}
$$

where $\wp=\frac{\pounds}{2}\left(1-\frac{\pounds}{2}\right)^{\frac{2-\pounds}{\pounds}}+\left(\frac{\bar{W}}{2}\right)^{1+\frac{\pounds}{2}},\wp_s=\frac{\pounds}{2}\left(1-\frac{\pounds}{2}\right)^{\frac{2-\pounds}{\pounds}}+\sum_{i=1}^{2}\left(\frac{\bar{W}_{si}}{2}\right)^{1+\frac{\pounds}{2}}$, $\left\|\mathrm{tr}\left(\frac{\tilde{W}^T\tilde{W}}{2}\right)\right\|\leq\bar{W}$, and $\left\|\mathrm{tr}\left(\frac{\tilde{W}_{si}^T\tilde{W}_{si}}{2}\right)\right\|\leq\bar{W}_{si}$ with $s=a,c$.

By choosing the suitable defined scales, one can ensure the relationship $\pounds T_c\sqrt{\omega_1\omega_2}\geq\max\left\{\omega_1\pi,9^{\pounds/2}\omega_2\pi\right\}$ holds. Then, substituting (66) and (67) into (65) and using Lemma 3 yields

$$
\begin{aligned}
\dot{V}\leq&-p_1\|e_1\|^{2-\pounds}-p_2\|e_1\|^{2+\pounds}-p_3\|e_2\|^{2-\pounds}\\
&-w_1\|\mathcal{S}\|^{2-\pounds}-p_4\|e_2\|^{2+\pounds}-w_2\|\mathcal{S}\|^{2+\pounds}\\
&-\left(\frac{h_1\tilde{\sigma}^2}{2}\right)^{\frac{2-\pounds}{2}}-\frac{2^{\frac{2+\pounds}{2}}h_2(1+\pounds)}{2+\pounds}\left(\frac{\tilde{\sigma}^2}{2}\right)^{\frac{2+\pounds}{2}}\\
&-\frac{\omega_1\pi}{\pounds T_c\sqrt{\omega_1\omega_2}}\left[\left(\frac{\tilde{W}^T\tilde{W}}{2}\right)^{\frac{2-\pounds}{2}}+\left(\sum_{i=1}^{2}\frac{\tilde{W}_{ai}^T\tilde{W}_{ai}}{2}\right)^{\frac{2-\pounds}{2}}\right.\\
&\left.+\left(\sum_{i=1}^{2}\frac{\tilde{W}_{ci}^T\tilde{W}_{ci}}{2}\right)^{\frac{2-\pounds}{2}}\right]\\
&-\frac{9^{\frac{\pounds}{2}}\omega_2\pi}{\pounds T_c\sqrt{\omega_1\omega_2}}\left[\left(\frac{\tilde{W}^T\tilde{W}}{2}\right)^{\frac{2+\pounds}{2}}+\left(\sum_{i=1}^{2}\frac{\tilde{W}_{ai}^T\tilde{W}_{ai}}{2}\right)^{\frac{2+\pounds}{2}}\right.\\
&\left.+\left(\sum_{i=1}^{2}\frac{\tilde{W}_{ci}^T\tilde{W}_{ci}}{2}\right)^{\frac{2+\pounds}{2}}\right]+\bar{\wp}\\
\leq&-\frac{\pi}{\pounds T_c\sqrt{\omega_1\omega_2}}\left(\omega_1V^{1-\frac{\pounds}{2}}+\omega_2V^{1+\frac{\pounds}{2}}\right)+\bar{\wp} \qquad (68)
\end{aligned}
$$

where $\bar{\wp}=\hbar_3+\wp+\wp_a+\wp_c$.

Consequently, it is obtained from (68) and Lemma 4 that the 2-DOF helicopter system is practically predefined-time stable. Furthermore, the tracking error will converge to a sufficiently small region, i.e.,

$$
\begin{aligned}
\Delta=\left\{\lim_{t\to T_p}e\mid V\leq\min\left\{\left(\frac{2\pounds T_c\sqrt{\omega_1\omega_2}}{\pi\omega_1}\right)^{\frac{2}{2-\pounds}},\right.\right.\\
\left.\left.\left(\frac{2\pounds T_c\sqrt{\omega_1\omega_2}}{\pi\omega_2}\right)^{\frac{2}{2+\pounds}}\right\}\right\} \qquad (69)
\end{aligned}
$$

within a predefined-time T_p that satisfies $T_p<T_{\max}=\sqrt{2}T_c$. Furthermore, in the light of the Lyapunov function of V,V_1

and V_2, we can get the filter error s and the estimation error $\tilde{\sigma}, \tilde{W}, \tilde{W}_{ai}$ and $\tilde{W}_{ci}$ are all bounded in predefined-time.

Remark 3. From a theoretical point of view, the desirable tracking performance depends on the defined scales $\pounds, T_c, \omega_1$, and ω_2. The minimum upper bound settling time of the system can be given in advance by tuning the control parameter T_c, and the decrease of T_c leads to a smaller settling time and convergence region. In addition, to enhance convergence accuracy and rate, $\pounds$, ω_1, and ω_2 could be selected as small as possible. However, it should be noticed that the decrease of the design parameters $\pounds, \omega_1, \omega_2, T_c$ will cause the increase of control gain. Thus, the tuning of design parameters needs to make a compromise between the convergence region and control gain through the trial-and-error tactic.

Furthermore, following the SETM (39), one has

$$\frac{d}{dt}|\chi(t)| = \frac{d}{dt}\sqrt{\chi^2(t)} \leq \dot{\chi}(t)\mathrm{sgn}(\chi(t)) \leq |\dot{\mu}(t)| \leq \mathcal{J}$$

where $\forall t \in [t_k, t_{k+1}]$, $\mathcal{J} > 0$ stands for a constant. According to the initial state $\chi(t_k) = 0$, yields $\lim_{t\to t_{k+1}} \chi(t_{k+1}) = \bar{\mathcal{J}}$, and

$$\bar{\mathcal{J}} = \max\left\{\frac{\upsilon_i|\mu_i(t)| + \Lambda_i}{\max\{\ell_i, |\dot{\mu}_i(t)|\}}, \zeta_1 e^{-\zeta_2 t} + \zeta_3\right\}.$$

Then, it is further obtained that

$$\frac{\chi(t_{k+1}) - \chi(t_k)}{t_{k+1} - t_k} \leq \mathcal{J},$$

and $T^* = t_{k+1} - t_k \geq \frac{\bar{\mathcal{J}}}{\mathcal{J}}$, in which T^* is trigger interval. In accordance with $\bar{\mathcal{J}} > 0$ and $\mathcal{J} > 0$, we can get $T^*_{\min} = \bar{\mathcal{J}}/\mathcal{J} > 0$. This also confirms that Zeno behavior can be excluded. ■

IV. Simulation Result

In this section, some simulation results are presented to demonstrate the validity and superiority of the proposed control method. The model parameters of 2-DOFHS [42] are displayed in Table I.

TABLE I: MODEL PARAMETERS

Symbol	Value	Unit	Symbol	Value	Unit
M	1.0750	kg	g	9.8	$\mathrm{m/s^2}$
D_p	0.0071	N/V	D_y	0.022	N/V
l_a	0.002	m	K_{pp}	0.0011	N·m/V
K_{py}	0.0021	N·m/V	K_{yp}	−0.0027	N·m/V
K_{yy}	0.0022	N·m/V	J_p	0.0215	$\mathrm{kg{\cdot}m^2}$
J_y	0.0237	$\mathrm{kg{\cdot}m^2}$			

Feasibility verification: For the investigated 2-DOFHS, the defined parameters are set as $\xi = 1, \omega_1 = \omega_2 = 1, \pounds = 2/59, T_c = 2, T_o = 1, w_{a1} = w_{a2} = 3, w_{c1} = w_{c2} = 10, b = b_1 = b_2 = b_4 = 0.01, b_3 = 0.1, \rho = 0.5, \varrho = 3, \Upsilon = 0.1 \times e^{-5t}, \upsilon_1 = \upsilon_2 = 0.7, \Lambda_1 = \Lambda_2 = 0.1, L_1 = L_2 = 3, \ell_1 = \ell_2 = 20, \zeta_1 = 0.9, \zeta_3 = 0.8, \zeta_2 = 0.01, \bar{\Lambda} = \zeta_4 = 2$. The configuration of the neural networks are given as: the basis functions are Gaussian functions (GFs) $\Phi(x) = \exp\left[(x - \upsilon_m)^T (x - \upsilon_m)/\aleph^2\right]$ and $\Phi_{si}(\mathcal{X}_i) = \exp\left[(\mathcal{X}_i - \upsilon_m)^T (\mathcal{X}_i - \upsilon_m)/\aleph^2\right]$ with input vectors $x = \left[G_1^T, G_2^T\right]^T, \mathcal{X}_1 = \left[e_1^T, \dot{G}_d^T\right]^T, \mathcal{X}_2 = \left[\mathcal{Q}^T, \hat{\mathcal{D}}^T, \mathcal{S}^T, e_2^T\right]^T$, the center vector $\upsilon_m = [-4, 4]$, and the width of the GFs $\aleph = 1$. The reference trajectory and uncertainty are chosen as $G_d = \left[\frac{\pi}{9}\sin(t), \frac{\pi}{18}\sin(t)\right]^T$ and $\mathcal{D} = [\sin(t), \cos(t)]^T + 0.1 * H(G)$. The initial conditions are given as $G(0) = [0.01, 0.01]^T\,(\mathrm{rad/s}), \hat{W}_{a1}(0) = \hat{W}_{a2}(0) = \mathrm{diag}\{0.2, 0.2\}, \hat{W}_{c1}(0) = \hat{W}_{c2}(0) = \mathrm{diag}\{0.1, 0.1\}, \hat{W}(0) = \mathrm{diag}\{0.2, 0.2\}$. The simulation results are displayed in Figs. 2-5. As can be seen from Fig. 2, the state variables θ and ϕ can track the desired trajectory θ_d and ϕ_d. Fig. 3 shows the response trajectories of tracking errors e_{11} and e_{12} with and without the disturbance observer. In addition, the curves of control signals V_p and V_y are plotted in Fig. 4. Furthermore, Fig. 5 depicts the trajectories of the norm of the actor-critic learning laws $\|\hat{W}_{aji}\|$ and $\|\hat{W}_{cji}\|(j = 1, 2, i = 1, 2)$. The estimation of lumped disturbance are depicted in Fig. 6. The triggered intervals under the proposed SETM and self-triggered mechanism (STM) developed in [25] are displayed in Figs. 7-8, where the controller update times under the SETM and STM are [656, 569] times and [824, 725] times, respectively.

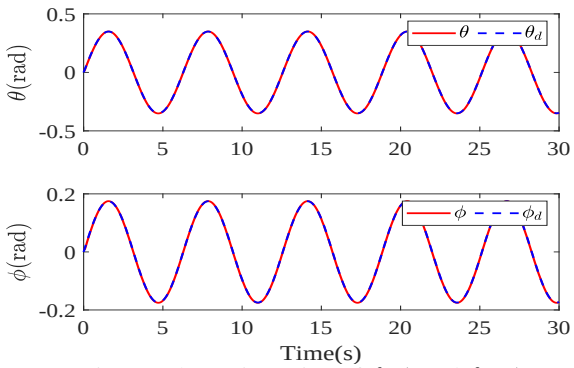

Fig. 2: The trajectories of θ, ϕ and θ_d, ϕ_d.

Comparative Analysis: Next, the some existing methods including NN-based adaptive finite-time control (NNBAFTC) in [31], the adaptive fuzzy fixed-time control (AFFITC) strategy in [33], and the adaptive nonsingular predefined-time control (ANPTC) in [51] are chosen to better demonstrate the merit of the proposed control method. Further, to assure the rigor of the comparison results, the external disturbances, design parameters, and initial conditions of the system are selected consistently. The comparison results are given by Figs. 9-11, where Fig. 9 plots the trajectories of the tracking errors $e_{1,i}(i = 1, 2)$ under different control strategies. The comparison results

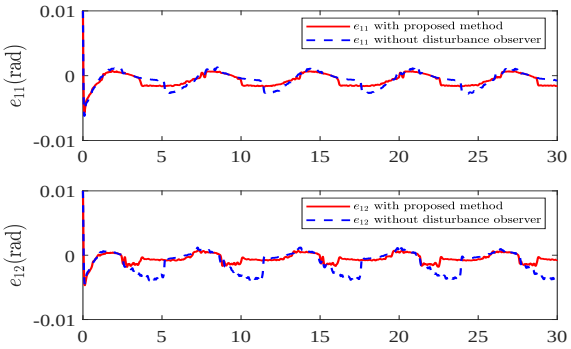

Fig. 3: The tracking errors $e_{1i}(i = 1, 2)$.

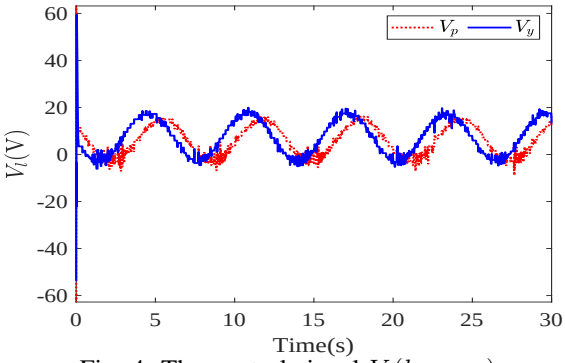

Fig. 4: The control signal $V_l(l = p, y)$.

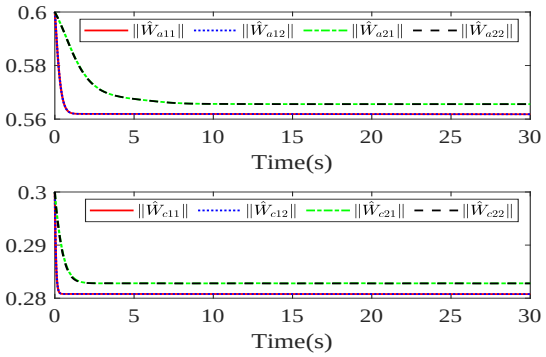

Fig. 5: Actor-critic NN weights.

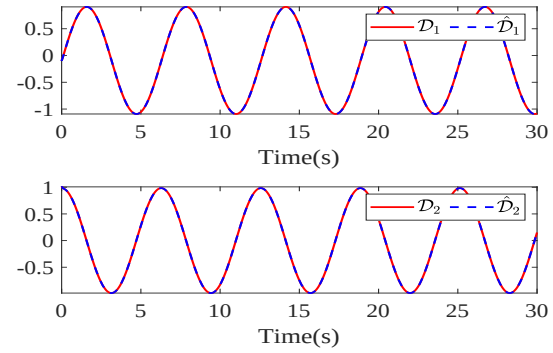

Fig. 6: The curves of composite disturbance $\mathcal{D}$ and its estimation $\hat{\mathcal{D}}$.

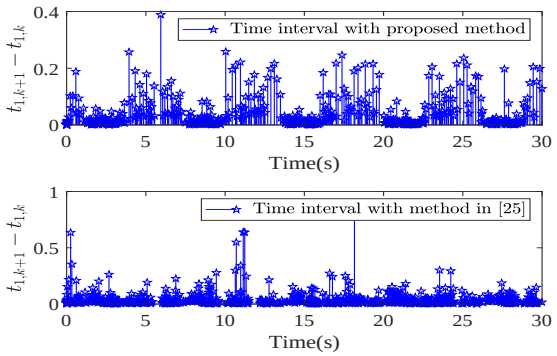

Fig. 7: Triggered intervals $t_{1,k+1} - t_{1,k}$.

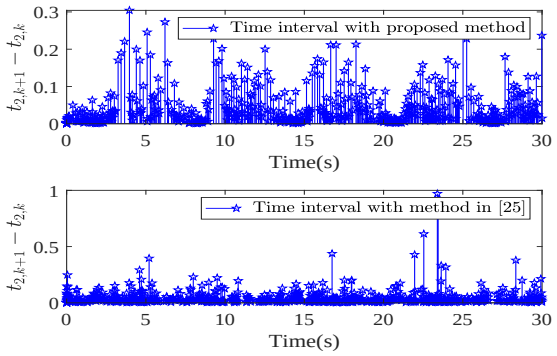

Fig. 8: Triggered intervals $t_{2,k+1} - t_{2,k}$.

about cost function $J = \int_0^{30} \left(e_1^T e_1 + \alpha^T \alpha + e_2^T e_2 + u^T u\right) dt$ under different methods are shown in Fig. 10. In addition, the performance indexes about mean absolute control action (MACA) $= \frac{1}{2t} \int_0^t |u_1(\tau)| + |u_2(\tau)| d\tau$, integral absolute error (IAE) $= \int_0^t |e_{1,i}| d\tau$, and integral time-weighted absolute error (ITAE) $= \int_0^t t|e_{1,i}| d\tau$ are adopted to quantitatively evaluation the control performance under different control schemes. Then, the quantitative data are illustrated more visually with the bar graphs in Fig. 11. According to Figs. 9-11, it is easily obtained that the proposed methods not only ensures better tracking performance, but also achieves an approximate trade-off between tacking performance and control costs.

V. Conclusion

In this paper, a reinforcement learning-based predefined-time adaptive optimal control strategy was developed for a 2-DOFHS via switching event-triggered communication. In the recursive control procedure, a PTNDO and a predefined-time filter were adopted to rapidly estimate the lumped disturbance and ensure the predefined-time convergence of the filter errors. Meanwhile, a SETM has been incorporated into

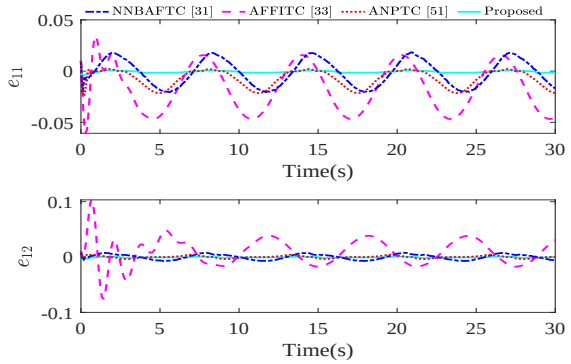

Fig. 9: The tracking error $e_{1i}(i = 1, 2)$ under different methods.

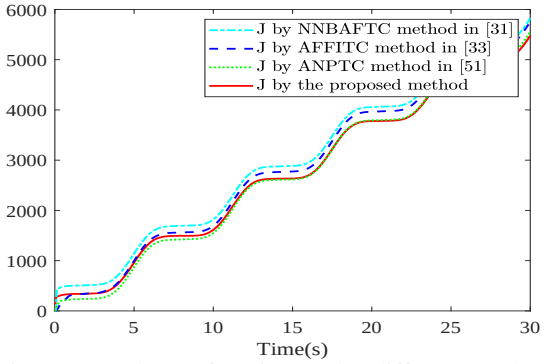

Fig. 10: Total cost function under different methods.

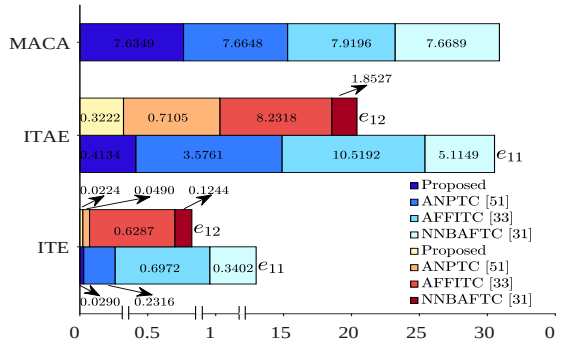

Fig. 11: Performance indexes MACA, ITAE, and IAE.

controller design, which can ensure a relatively satisfactory tracking performance while achieving the balance between data transmission and control expenses. The obtained results have indicated that the proposed control strategy could ensure that all the signals in the CLS are practically predefined-time bounded. Finally, the superiority and effectiveness of the proposed control strategy have been verified through the simulation results. In view of the significance of system security, how to carry out security analysis and develop a safety-critical optimized learning control solution integrated with control barrier function and control Lyapunov function for a 2-DOFHS will be one of our key research contents in the future.

REFERENCES

[1] Y.-C. Lai and T.-Q. Le, "Adaptive learning-based observer with dynamic inversion for the autonomous flight of an unmanned helicopter," *IEEE Trans. Aerospace. Electronic systems*, vol. 57, no. 3, pp. 1803–1814, Jun. 2021.

[2] S. K. Kim, K. S. Kim, and C. K. Ahn, "Order reduction approach to velocity sensorless performance recovery PD-type attitude stabilizer for 2-DOF helicopter applications," *IEEE Trans. Industrial Info.*, vol. 18, no. 10, pp. 6848–6856, Oct. 2022.

[3] B. Xian, X. Zhang, H. Zhang, and X. Gu, "Robust adaptive control for a small unmanned helicopter using reinforcement learning," *IEEE Trans. Neural Networks and Learning Syst.*, vol. 33, no. 12, pp. 7589–7597, Dec. 2022.

[4] T. Zou, H. Yang, G. Ma, Z. Li, S. Liu, and Z. Zhao, "Adaptive constrained control for two-degree-of-freedom helicopter system with actuator faults," *IEEE Trans. Aerospace. Electronic systems*, vol. 60, no. 5, pp. 6363–6375, Oct. 2024.

[5] J. Wang, Y. Yi, J. Yang, and W. Zheng, "Dynamic double event-triggered anti-disturbance tracking control for a 2-DOF small unmanned helicopter," *IEEE Trans. Cybernet.*, vol. 54, no. 10, pp. 6256–6268, Oct. 2024.

[6] M. Chen, K. Yan, and Q. Wu, "Multiapproximator-based fault-tolerant tracking control for unmanned autonomous helicopter with input saturation," *IEEE Trans. Syst. Man Cybernet. Syst.*, vol. 52, no. 9, pp. 5710–5722, Sep. 2022.

[7] Z. Zhao, J. Zhang, Z. Liu, C. Mu, and K. S. Hong, "Adaptive neural network control of an uncertain 2-DOF helicopter with unknown backlash-like hysteresis and output constraints," *IEEE Trans. Neural Networks and Learning Syst.*, vol. 34, no. 12, pp. 10 018–10 027, Dec. 2023.

[8] H. Ma, M. Chen, G. Feng, and Q. Wu, "Disturbance-observer-based adaptive fuzzy tracking control for unmanned autonomous helicopter with flight boundary constraints," *IEEE Trans. Fuzzy Syst.*, vol. 31, no. 1, pp. 184–198, Jan. 2023.

[9] G. Qi, X. Li, and Z. Chen, "Problems of extended state observer and proposal of compensation function observer for unknown model and application in UAV," *IEEE Trans. Syst. Man Cybernet. Syst.*, vol. 52, no. 5, pp. 2899–2910, May. 2022.

[10] H. Ma, M. Chen, and Q. Wu, "Disturbance observer-based safe tracking control for unmanned helicopters with partial state constraints and disturbances," *IEEE/CAA J. Automat. Sinica*, vol. 10, no. 11, pp. 2056–2069, Nov. 2023.

[11] D. Wang, Q. Zong, B. Tian, S. Shao, X. Zhang, and X. Zhao, "Neural network disturbance observer-based distributed finite-time formation tracking control for multiple unmanned helicopters," *ISA T*, vol. 73, pp. 208–226, Feb. 2018.

[12] T. Xie, B. Xian, X. Gu, J. Hu, and M. Liu, "Disturbance observer-based fixed-time tracking control for a tilt trirotor unmanned aerial vehicle," *IEEE Trans. Industrial Elec.*, vol. 71, no. 4, pp. 3894–3903, Apr. 2024.

[13] R. Bellman, "Dynamic programming," *Science*, vol. 153, no. 3731, pp. 34–37, Jul. 1966.

[14] D. Li and J. Dong, "Approximate optimal robust tracking control based on state error and derivative without initial admissible input," *IEEE Trans. Syst. Man Cybernet. Syst.*, vol. 54, no. 2, pp. 1059–1069, Feb. 2024.

[15] Z. Zhao, W. He, C. Mu, T. Zou, K. S. Hong, and H. Li, "Reinforcement learning control for a 2-DOF helicopter with state constraints: Theory and experiments," *IEEE Trans. Autom. Sci. Eng.*, vol. 21, no. 1, pp. 157–167, Jan. 2024.

[16] L. Cao, Y. Qin, Y. Pan, and H. Liang, "Prescribed performance-based optimal formation control for USVs with position constraints and yaw angle time-varying partial constraints," *IEEE Trans. Intell. Transp. Syst.*, vol. 26, no. 3, pp. 4109–4121, Mar. 2025.

[17] G. K. Vamvoudakis and L. L. Frank, "Online actor-critic algorithm to solve the continuous-time infinite horizon optimal control problem," *Automatica*, vol. 46, no. 5, pp. 878–888, May. 2010.

[18] H. Liu, Y. Pan, J. Cao, H. Wang, and Y. Zhou, "Adaptive neural network backstepping control of fractional-order nonlinear systems with actuator faults," *IEEE Trans. Neural Networks and Learning Syst.*, vol. 31, no. 12, pp. 5166–5177, Dec. 2020.

[19] X. Yang, M. Xu, and Q. Wei, "Dynamic event-sampled control of interconnected nonlinear systems using reinforcement learning," *IEEE Trans. Neural Networks and Learning Syst.*, vol. 35, no. 1, pp. 923–937, Jan. 2024.

[20] G. Zhang and Q. Zhu, "Event-triggered optimized control for nonlinear delayed stochastic systems," *IEEE Trans. Circuits Syst. I, Reg. Papers*, vol. 68, no. 9, pp. 3808–3821, Sep. 2021.

[21] H. Zhu, Y. Li, and S. Tong, "Dynamic event-triggered reinforcement learning control of stochastic nonlinear systems," *IEEE Trans. Fuzzy Syst.*, vol. 31, no. 9, pp. 2917–2928, Sep. 2023.

[22] K. Yu, Y. Li, Z. Peng, and S. Tong, "Distributed event-triggered formation control of planar vehicles without velocity sensors," *IEEE Trans. Veh. Technol.*, vol. 72, no. 3, pp. 2988–3000, Mar. 2023.

[23] D. Li and J. Dong, "Fuzzy weight-based reinforcement learning for event-triggered optimal backstepping control of fractional-order nonlinear systems," *IEEE Trans. Fuzzy Syst.*, vol. 32, no. 1, pp. 214–225, Jan. 2024.

[24] L. Cao, Y. Pan, H. Liang, and C. K. Ahn, "Event-based adaptive neural network control for large-scale systems with nonconstant control gains and unknown measurement sensitivity," *IEEE Trans. Syst. Man Cybernet. Syst.*, vol. 54, no. 11, pp. 7027–7038, Nov. 2024.

[25] J. Wang, H. Zhang, K. Ma, Z. Liu, and C. L. P. Chen, "Neural adaptive self-triggered control for uncertain nonlinear systems with input hysteresis," *IEEE Trans. Neural Networks and Learning Syst.*, vol. 33, no. 11, pp. 6206–6214, Nov. 2022.

[26] J. Wu, F. He, H. Shen, S. Ding, and Z. Wu, "Adaptive NN fixed-time fault-tolerant control for uncertain stochastic system with deferred output constraint via self-triggered mechanism," *IEEE Trans. Cybernet.*, vol. 53, no. 9, pp. 5892–5903, Sep. 2023.

[27] L. Wang and J. Dong, "Adaptive fuzzy consensus tracking control for uncertain fractional-order multi-agent systems with event-triggered input," *IEEE Trans. Fuzzy Syst.*, vol. 30, no. 2, pp. 310–320, Feb. 2022.

[28] H. Zhang, X. Guo, J. Sun, and Y. Zhou, "Event-triggered cooperative adaptive fuzzy control for stochastic nonlinear systems with measurement sensitivity and deception attacks," *IEEE Trans. Fuzzy Syst.*, vol. 31, no. 3, pp. 774–785, Mar. 2023.

[29] X. Wang, Z. Li, X. Yu, and Z. He, "Adaptive smooth disturbance observer-based fast finite-time attitude tracking control of a small unmanned helicopter," *J. Franklin Inst.*, vol. 359, no. 11, pp. 5322–5340, Jul. 2022.

[30] Y. Ren, D. Liu, Z. Zhao, and C. K. Ahn, "Finite-time anti-disturbance control of an information-constrained autonomous helicopter flexible slung-load system with compound disturbance," *Aerosp. Sci. Technol.*, vol. 140, Sep. 2023, Art. no. 108417.

[31] Z. Zhao, J. Zhang, S. Chen, W. He, and K. S. Hong, "Neural-network-based adaptive finite-time control for a two-degree-of-freedom helicopter system with an event-triggering mechanism," *IEEE/CAA J. Automat. Sinica*, vol. 10, no. 8, pp. 1754–1765, Aug. 2023.

[32] Z. Zhao, J. Wu, C. Mu, Y. Liu, and K. S. Hong, "Neural-network-based adaptive fixed-time control for a 2-DOF helicopter system with input quantization and output constraints," *IEEE Trans. Neural Networks and Learning Syst.*, to be published, doi: 10.1109/TNNLS.2024.3403145.

[33] H. Ma, R. Ren, F. Tao, Z. Fu, and N. Wang, "FTDO-based adaptive fuzzy fixed-time tracking control for uncertain unmanned helicopter with output constraints," *Aerosp. Sci. Technol.*, vol. 147, Apr. 2024, Art. no. 109019.

[34] H. Shen, X. Yu, H. Yan, J. H. Park, and J. Wang, "Robust fixed-time sliding mode attitude control for a 2-DOF helicopter subject to input saturation and prescribed performance," *IEEE Trans. Transport. Electrific.*, vol. 11, no. 1, pp. 1223–1233, Feb. 2025.

[35] J. D. Sánchez-Torres, E. N. Sanchez, and A. G. Loukianov, "Predefined-time stability of dynamical systems with sliding modes," in *Proc. Amer. Control Conf. (ACC),* 2015, pp. 5842–5846.

[36] S. Yang, Y. Pan, L. Cao, and L. Chen, "Predefined-time fault-tolerant consensus tracking control for multi-UAV systems with prescribed performance and attitude constraints," *IEEE Trans. Aerospace. Electronic systems*, vol. 60, no. 4, pp. 4058–4072, Aug. 2024.

[37] H. Shen, W. Zhao, J. Cao, J. H. Park, and J. Wang, "Predefined-time event-triggered tracking control for nonlinear servo systems: A fuzzy weight-based reinforcement learning scheme," *IEEE Trans. Fuzzy Syst.*, vol. 32, no. 8, pp. 4557–4569, Aug. 2024.

[38] T. Zhang, R. Bai, and Y. Li, "Practically predefined-time adaptive fuzzy quantized control for nonlinear stochastic systems with actuator dead zone," *IEEE Trans. Fuzzy Syst.*, vol. 31, no. 4, pp. 1240–1253, Apr. 2023.

[39] X. Song, L. Chu, Z. Zhao, S. Song, and K. S. Hong, "Predefined-time neural adaptive quantized self-triggered control with appointed performance for a 2-DOF helicopter system," *IEEE Trans. Veh. Technol.*, vol. 74, no. 6, pp. 8608–8618, Jun. 2025.

[40] X. Song, P. Sun, C. K. Ahn, and S. Song, "Reinforcement learning-based event-triggered predefined-time optimal fuzzy control for nonlinear constrained systems," *IEEE Trans. Fuzzy Syst.*, vol. 32, no. 8, pp. 4646–4659, Aug. 2024.

[41] Z. Zhao, J. Wu, Z. Liu, W. He, and C. L. P. Chen, "Adaptive neural network control of a 2-DOF helicopter system considering input constraints and global prescribed performance," *Sci. China Inform. Sci.*, vol. 67, Jun. 2024, Art. no. 172202.

[42] Z. Zhao, J. Zhang, Z. Liu, W. He, and K. S. Hong, "Adaptive quantized fault-tolerant control of a 2-DOF helicopter system with actuator fault and unknown dead zone," *Automatica*, vol. 148, Feb. 2023, Art. no. 110792.

[43] Q. Inc., "Quanser AERO laboratory guide," *Technical Report*, Quanser 2016.

[44] S. P. Sadala and B. M. Patre, "A new continuous sliding mode control approach with actuator saturation for control of 2-DOF helicopter system," *ISA T*, vol. 74, pp. 165–174, Mar. 2018.

[45] M. Chen, P. Shi, and C. C. Lim, "Adaptive neural fault-tolerant control of a 3-DOF model helicopter system," *IEEE Trans. Syst. Man Cybernet. Syst.*, vol. 46, no. 2, pp. 260–270, Feb. 2016.

[46] M. M. Polycarpou, "Stable adaptive neural control scheme for nonlinear systems," *IEEE Trans. Automat. Control*, vol. 41, no. 3, pp. 447–451, Mar. 1996.

[47] S. Song, J. H. Park, B. Zhang, and X. Song, "Adaptive NN finite-time resilient control for nonlinear time-delay systems with unknown false data injection and actuator faults," *IEEE Trans. Neural Networks and Learning Syst.*, vol. 33, no. 10, pp. 5416–5428, Oct. 2022.

[48] G. H. Hardy, J. E. Littlewood, and G. Polya, *Inequalities*. London, U.K.: Cambridge Univ. Press, 1952.

[49] S. Xie, Q. Chen, and Q. Yang, "Adaptive fuzzy predefined-time dynamic surface control for attitude tracking of spacecraft with state constraints," *IEEE Trans. Fuzzy Syst.*, vol. 31, no. 7, pp. 2292–2304, Jul. 2023.

[50] Y. Sun and L. Zhang, "Fixed-time adaptive fuzzy control for uncertain strict feedback switched systems," *Inf. Sci.*, vol. 546, pp. 742–752, Feb. 2021.

[51] S. Xie and Q. Chen, "Adaptive nonsingular predefined-time control for attitude stabilization of rigid spacecrafts," *IEEE Trans. Circuits Syst. II, Exp. Briefs*, vol. 69, no. 1, pp. 189–193, Jan. 2022.

Xiaona Song (Senior Member, IEEE) received the Ph.D. degree in Control Science and Engineering from Nanjing University of Science and Technology, Nanjing, China, in 2011. From Feb. 2009 to Aug. 2009, Apr. 2016 to Apr. 2017 and July 2019 to Aug. 2019, she was a visiting scholar with the Department of Electrical Engineering, Utah State University, Southern Illinois University Carbondale, and Yeungnam University , respectively. Since 2011, she has been with Henan University of Science and Technology, Luoyang, China, where she is currently a Professor with the School of Information Engineering.

Her current research interests include reaction-diffusion systems, adaptive and learning control of flexible systems, cooperative control and optimization of unmanned systems.

Longbo Chu received the B.S. degree in electronic science and technology from the School of Mechanical and Electrical Engineering, Henan Institute of Science and Technology, Xinxiang, China, in 2022. He is currently pursuing the Master degree in control engineering with the School of Information Engineering, Henan University of Science and Technology, Luoyang, China

His current research interests include adaptive and learning control for unmanned helicopter systems.

Zhijia Zhao (Member, IEEE) received his B. Eng. degree in automatic control from North China University of Water Resources and Electric Power, Zhengzhou, China, in 2010, and his M.Eng. and Ph.D. degree in automatic control from South China University of Technology, Guangzhou, China, in 2013 and 2017, respectively.

He is currently a professor in the School of Mechanical and Electrical Engineering, Guangzhou University. His research interests include adaptive and learning control, flexible mechanical systems, and robotics.

Keum-Shik Hong (Life Fellow, IEEE) received his B.S. degree in Mechanical Design and Production Engineering from Seoul National University in 1979, his M.S. degree in Mechanical Engineering from Columbia University, New York, in 1987, and both an M.S. degree in Applied Mathematics and a Ph.D. in Mechanical Engineering from the University of Illinois at Urbana-Champaign in 1991.

He was with the School of Mechanical Engineering, Pusan National University during 1993-2022, and is a Professor Emeritus since 2022. His Integrated Dynamics and Control Engineering Laboratory was a National Research Laboratory designated by the Ministry of Science and Technology of Korea in 2003. In 2009, under the auspices of the World Class University Program of the Ministry of Education, Science, and Technology of Korea, he established the Department of Cogno-Mechatronics Engineering, PNU. He holds a Distinguished Professorship from the Institute For Future, School of Automation, Qingdao University, Qingdao, China.

He is an IEEE Fellow, a Fellow of the Korean Academy of Science and Technology, an ICROS Fellow, a Member of the National Academy of Engineering of Korea, and many other societies. Dr. Hong served as Associate Editor of Automatica (2000-2006) and an Editor-in-Chief of the Journal of Mechanical Science and Technology (JMST, 2008-2011) and the International Journal of Control, Automation, and Systems (IJCAS, 2018-2022). He was a past President of the Institute of Control, Robotics and Systems (ICROS), Korea, and the Asian Control Association (2020-21). Dr. Hong received the Presidential Award of Korea (2007) and the Service Merit Medal of Korea (2022) from the Korean government. His academic awards include the Best Paper Award from the KFSTS of Korea (1999), the IEEE Academic Award (2016), etc. His current research interests include autonomous vehicles, brain-computer interface, nonlinear systems theory, adaptive control, distributed parameter systems, and innovative control applications in brain engineering.

Shuai Song (Member, IEEE) received the M.S. degree in Control Engineering from Henan University of Science and Technology, Luoyang, China, in 2017, and the Ph.D. degree in Control Science and Engineering from Nanjing University of Science and Technology, Nanjing, China, in 2021. From April 2019 to November 2020, he was a visiting scholar with the Department of Electrical Engineering, Yeungnam University, Republic of Korea. Since 2021, he has been with Henan University of Science and Technology, Luoyang, China, where he is currently an Associate Professor with the School of Information Engineering.

His current research interests include adaptive and learning control for nonlinear systems, cooperative formation control of unmanned systems.